

SRAGAN: Saliency Regularized and Attended Generative Adversarial Network for Chinese Ink-wash Painting Generation

Xiang Gao¹ and Yuqi Zhang^{2*}

¹School of Computer Science & Technology, University of Chinese Academy of Sciences, 19A Yuquan Road, Beijing, 100049, China.

²School of Mathematical Sciences, University of Chinese Academy of Sciences, 19A Yuquan Road, Beijing, 100049, China.

*Corresponding author(s). E-mail(s):

zhangyuqi201@mailsucas.ac.cn;

Contributing authors: gaoxiang181@mailsucas.ac.cn;

Abstract

This paper handles the problem of converting real pictures into traditional Chinese ink-wash paintings, i.e., Chinese ink-wash painting style transfer. Though this problem could be realized by a wide range of image-to-image translation models, a notable issue with all these methods is that the original image content details could be easily erased or corrupted due to transfer of ink-wash style elements. To solve or ameliorate this issue, we propose to incorporate saliency detection into the unpaired image-to-image translation framework to regularize content information of the generated paintings. The saliency map is utilized for content regularization from two aspects, both explicitly and implicitly: (i) we propose saliency IOU (SIOU) loss to explicitly regularize saliency consistency before and after stylization; (ii) we propose saliency adaptive normalization (SANorm) which implicitly enhances content integrity of the generated paintings by injecting saliency information to the generator network to guide painting generation. Besides, we also propose saliency attended discriminator network which harnesses saliency mask to focus generative adversarial attention onto salient image regions, it contributes to producing finer ink-wash stylization effect for salient objects of images. Qualitative and quantitative experiments consistently demonstrate superiority of our model over related advanced methods for Chinese ink-wash painting style transfer.

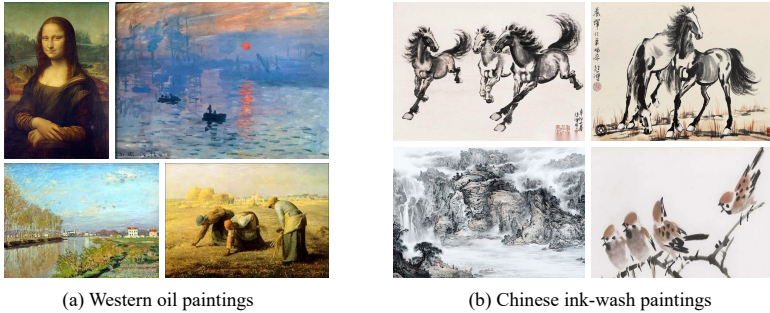


Fig. 1 Comparison of Western oil paintings and traditional Chinese ink-wash paintings.

Keywords: Style transfer, Generative adversarial networks, Chinese ink-wash painting, Regularization

1 Introduction

Chinese ink-wash painting is a representative art form in Chinese traditional culture. As compared and shown in Fig. 1, Chinese ink-wash paintings differ substantially from western paintings mainly in two aspects. (i) They are created by painting onto a canvas of paper or silk with a brush dipped with ink and water, rather than using pigments as western paintings. (ii) Chinese ink-wash paintings often feature landscapes, animals, birds, etc., they do not emphasize a precise depiction of scenes or objects, but instead the skills of applying ink and the emotional statement of the painter.

The growing prosperity of artificial intelligence has been revolutionizing many computer vision fields, e.g., image and video understanding [1][2], detection [3][4], segmentation [5][6], restoration [7][8], etc. Among various domains assisted with AI technologies there is also the artistic one. Actually, AI based automatic art creation has been receiving increasing attention recent years, leading to a proliferation of AI art generation tools and services, behind which neural style transfer algorithms [9] and generative adversarial networks (GANs) [10] are the main force of related technologies.

Style transfer technologies date back to the seminal work of Gatys et al. [9], which for the first time utilize convolutional neural network to separate and recombine image content and style, achieving impressive success in reproducing artistic painting styles onto natural pictures. Afterwards, extensive efforts have been made to improve style transfer algorithm in visual quality [11][12][13], inference speed [14][15], and extension to more styles [16][17][18][19]. Until now, remarkable progresses in style transfer problem have been made. Advanced methods [20][21][22][23] are able to transfer arbitrary styles from any reference images onto any source pictures instantly with high visual quality. When used for artistic painting synthesis, neural style transfer methods are often

limited to paintings with prominent textures, since these methods resort to texture descriptor based style losses which essentially transfer low-level texture features, not capable of capturing more abstract high-level styles.

By virtue of inherent advantage of GANs in latent distribution learning, Elgammal et al. [24] pioneered using GAN to create “art”. Later on, GAN based image-to-image translation methods have been increasingly dominating artistic painting generation problem. These methods can be divided into supervised and unsupervised ones according to whether paired training data of source and target domains exist. In supervised setting, some work utilizes conditional GAN [25] framework to generate high-quality portrait sketches [26][27] or artistic portrait paintings [28]. Due to the cost and difficulty of collecting paired training data, unsupervised methods are practically more feasible. Typical works include unidirectional GAN models [29][30] that transfer painting styles with adversarial learning and maintain image content via perceptual loss [14] related constraints, as well as bidirectional GAN models [31][32][33] that establish mutual cross-domain mappings with two GANs and preserve image content through cycle-consistency related constraints.

Nevertheless, attention of painting style transfer has almost been paid on western painting styles. In this paper, we focus on transforming real pictures into Chinese ink-wash paintings, which is still a less concerned problem. Our method is built upon bidirectional image-to-image translation architecture based on our empirical observation that bidirectional GAN framework is noticeably better at capturing ink-water effect than unidirectional GAN structure. One notable issue with this task is that the generated ink-wash paintings suffer from content corruption (e.g., missing and distortion of object details, redundant textures and lines) caused by translation of ink-wash style elements. How to faithfully preserve object fine structures without weakening ink-wash stylization strength is a challenging issue.

Established on CycleGAN [31], the classical unsupervised cross-domain image translation framework, He et al. [34] propose ChipGAN tailored specifically for Chinese ink-wash painting style transfer. ChipGAN proposes a brush stroke constraint for better preserving object outlines. Specifically, they introduce an edge detection model [35] to detect object contours and enforce contour consistency before and after style translation. However, we argue that mild shift of object contours is reasonable due to the specific brushwork characteristics of Chinese ink-wash painting, while enforcing object saliency consistency is a more effective alternative to encourage generation of fine structures of image objects.

Observing that distortion or missing of content information could cause noticeable difference on image saliency maps. We consider utilizing such sensitivity of visual saliency to object content integrity to regularize content preservation. Besides, it is intuitive that the salient object in real photo manifold should also be visually salient in generated paintings. Therefore, we propose to introduce saliency detection [36] into unpaired image-to-image translation for saliency regularized Chinese ink-wash painting style transfer.

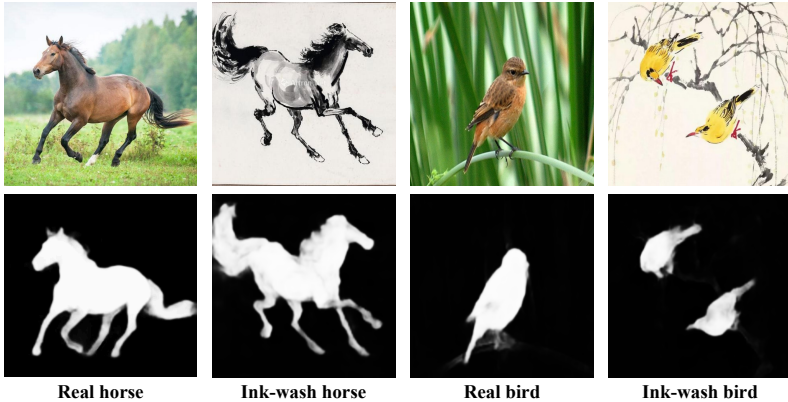


Fig. 2 Top: real-world images and Chinese ink-wash paintings. Bottom: saliency maps detected by CSNet [36]. The saliency detection deep model pretrained on real-world images can also segment out salient objects well in Chinese ink-wash paintings.

Moreover, the detected saliency maps also provide clues for vision attention. It indicates where the salient objects are, i.e., where the stylization should be focused on. The remaining question is that, is saliency detection model trained on real-world images also effective for Chinese ink-wash paintings? The answer is yes. We evaluate the pretrained saliency detection model CSNet [36] on both real pictures and Chinese ink-wash paintings, example results shown in Fig. 2 indicate that pretrained saliency detection model can also segment out salient objects well for Chinese ink-wash paintings. Based on the above motivations and observations, we propose saliency regularized and attended generative adversarial network (SRAGAN) for Chinese ink-wash painting generation. Our contributions can be summarized as follows:

- We propose saliency IOU (SIOU) loss which explicitly alleviates content corruption issue by regularizing object saliency consistency before and after ink-wash stylization.
- We propose saliency regularized generator, which implicitly relieves content corruption issue by incorporating saliency guiding information into the generator with our proposed saliency adaptive normalization (SANorm).
- We propose saliency attended discriminator, which brings finer ink-wash stylization effect by utilizing saliency masks to guide generative adversarial learning attention onto salient objects of images.

2 Related Work

2.1 Style Transfer

Gatys et al. [9] first propose using Gram matrix to represent image style, opening the door of neural style transfer (NST). Later on, the algorithm is speeded up by training a feedforward network [14][15]. Meanwhile, more style losses have been designed, e.g., MMD loss [38], relaxed EMD loss [39], CNNMRF

loss [40], contextual loss [41], etc. Some work extend NST to multiple styles with diversified stylization filters [16], conditional instance normalization [17], or conditional signal injection [18]. Subsequently, arbitrary fast style transfer is enabled with dynamic feature statistics adjusting layers, e.g., AdaIN [37], WCT [42]. More recent advances in arbitrary style transfer include combination with attention mechanism [23][43] or contrastive learning [21][22][44].

2.2 Image-to-image Translation

Image-to-image translation is a typical application of GAN in image processing. PixPix [25] establishes a conditional GAN framework for supervised cross-domain translation tasks with paired training data. Its derived applications include font style transfer [45][46] and portrait style transfer [26][28]. In unsupervised setting, methods have been proposed to realize cross-domain translation with unpaired data through cycle-consistency constraint (e.g., CycleGAN [31]), shared latent space assumption (e.g., UNIT [47]), self-supervised constraint (e.g., GcGAN [48], DistanceGAN [49]), contrastive learning (e.g., CUT [50]). Advances in unsupervised methods extremely enrich style transfer applications, such as makeup style transfer [51][52][53], painting style transfer [28][34][54], cartoon style transfer [55][56][57], etc.

3 Method

Our SRAGAN model is built upon a bidirectional GAN framework which establishes mutual translation mappings between source and target domains. Let X be the source domain of real images, Y be the target domain of Chinese ink-wash paintings, the model is trained with a randomly sampled image pair $\{x \in X, y \in Y\}$ at each training iteration, and is inferred by feeding in a real image to obtain the generated Chinese ink-wash painting via the learned source-to-target translation mapping.

3.1 Overall Architecture

As illustrated in Fig. 3, the generator G transforms a source-domain real image $x \in X$ into a target-domain painting $x' = G(x) \in Y$, and the generator F inversely learns to translate a target-domain painting $y \in Y$ into a source-domain real image $y' = F(y) \in X$. The target-domain discriminator D_Y acts as an adversary against the generator G by discriminating synthesized paintings from real target-domain paintings. Similarly, the source-domain discriminator D_X adversarially learns to distinguish the output results of F from real source-domain images. Such adversarial learning endows the generator G and F painting stylization and de-stylization ability respectively. Meantime, cycle-consistency constraint is used to avoid cross-domain translation content mismatch by enforcing mutual invertibility of two generators, i.e., $x \approx \hat{x} = F(x') = F(G(x))$; $y \approx \hat{y} = G(y') = G(F(y))$.

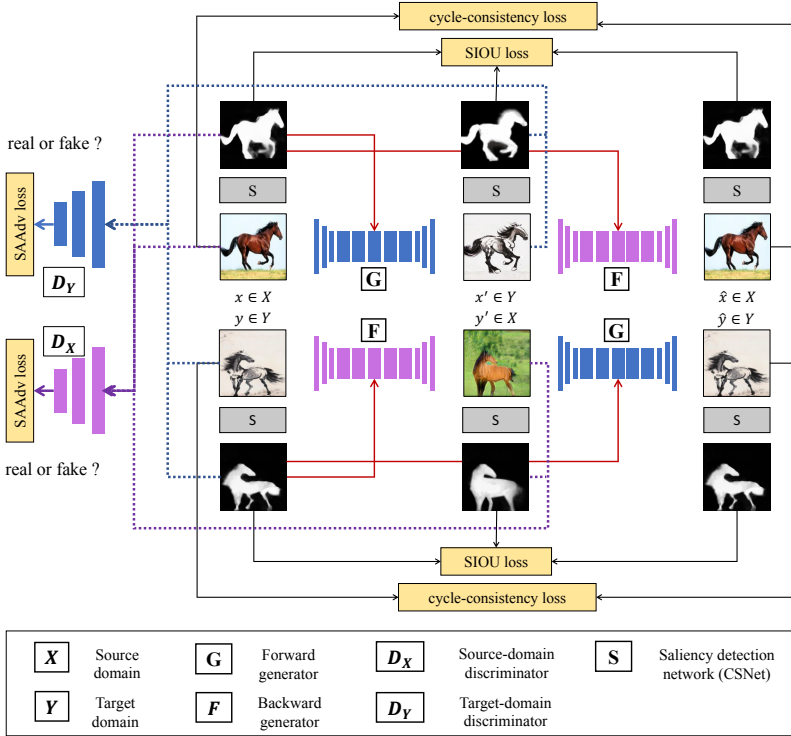


Fig. 3 Overall architecture of our SRAGAN model. It is composed of a forward GAN (comprising generator G and target-domain discriminator D_Y) mapping from source domain X to target domain Y , and a backward GAN (comprising generator F and source-domain discriminator D_X) for inverse mapping from Y to X . The saliency maps provided by saliency detection model are incorporated into both generators and discriminators for saliency regularized generation and saliency attended discrimination, respectively. The two GANs are coupled with cycle-consistency loss and our proposed SIOU loss.

To alleviate the problem of content corruption as well as improving style transfer quality, we incorporate saliency detection into the above basic framework for saliency regularized and attended generative adversarial learning. The pretrained saliency detection model S is introduced to produce saliency maps which highlight regions of salient objects in a picture or painting. Such saliency information is utilized to improve style transfer quality from three aspects. (1) We design saliency regularized generator which introduces saliency information to guide generator forward propagation via our proposed SANorm layer. (2) We explicitly enforce object saliency consistency before and after ink-wash style translation via our proposed saliency IOU (SIOU) loss. (3) We design saliency attended discriminator which employs saliency masks to focus more attention of generative adversarial learning onto salient objects of images.

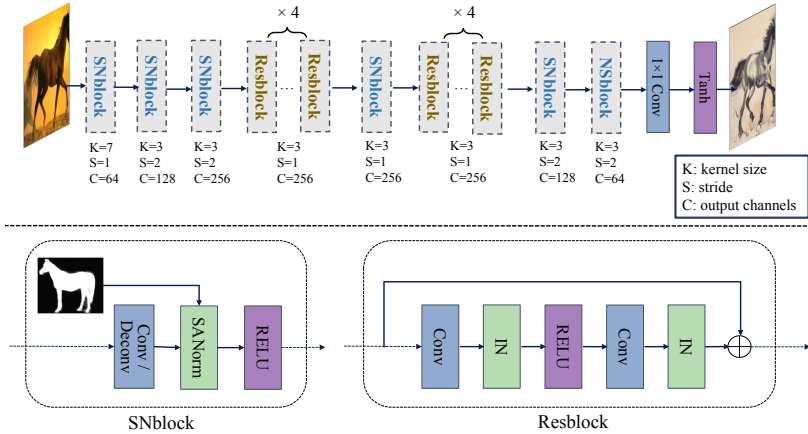


Fig. 4 Architecture details of our proposed saliency regularized generator.

3.2 Model Components

In our SRAGAN model, we use the pretrained CSNet [36], a lightweight saliency detection model, to perform saliency detection. Below is the detailed description of our saliency based generator and discriminator networks.

3.2.1 Saliency Regularized Generator

The architecture details of our proposed saliency regularized generator is illustrated in Fig. 4. It starts with a downsampling stage (comprising three convolutional blocks) which downsamples input images to $1/4$ spatial size and increases channel dimension to 256. Then it comes to a feature learning stage comprising 9 convolutional blocks with feature resolution and channel dimension unchanged. At last, an upsampling stage (comprising two deconvolutional blocks and a final 1×1 convolutional layer) upsamples feature maps back into the original image shape. There are two types of convolutional blocks in our generator network: residual convolutional block (Resblock) and saliency normalized convolutional block (SNblock). In all Resblocks, instance normalization (IN) is used to accelerate learning of target style distribution. In SNblocks, the kernel ingredient is our proposed saliency adaptive normalization (SANorm) layer, it learns to adaptively infuse structure information from the detected saliency maps into the current convolutional features as content structure guidance. All the convolutional blocks at downsampling and upsampling stage as well as the middle block at feature learning stage are our proposed SNblocks, while the rest are the normal Resblocks.

In SNblock, we propose SANorm to adaptively modulate convolutional features with saliency maps to enhance preservation of object content structure. The SANorm is illustrated in Fig. 5. Suppose the input feature of SANorm is f^{in} with shape $\{C, H, W\}$, where C denotes channel dimension, H and W are feature height and width respectively. Firstly, the input feature is normalized

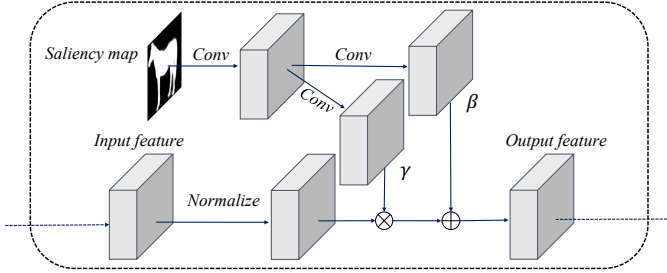


Fig. 5 Illustration of saliency adaptive normalization (SANorm) layer.

across spatial dimension to standard Gaussian distribution, i.e.,

$$\tilde{f}_{c,h,w}^{in} = \frac{f_{c,h,w}^{in} - \mu_c}{\sigma_c}, \quad (1)$$

where c, h, w are indices along channel, height, and width dimension. μ_c and σ_c are mean and standard deviation of the c th channel of f^{in} , i.e.,

$$\mu_c = \frac{1}{HW} \sum_{h,w} f_{c,h,w}^{in}, \quad \sigma_c = \sqrt{\frac{1}{HW} \sum_{h,w} (f_{c,h,w}^{in} - \mu_c)^2}. \quad (2)$$

Then, the normalized feature \tilde{f}^{in} is modulated with an elementwise multiplication and an elementwise addition, obtaining the output feature f^{out} :

$$f^{out} = \tilde{f}^{in} \times \gamma + \beta, \quad (3)$$

where γ and β are scaling tensor and shifting tensor that have the same shape with the input feature f^{in} . They are learned from an input saliency map S with two sibling convolutional branches g_1 and g_2 , i.e.,

$$\gamma = g_1(S), \quad \beta = g_2(S), \quad (4)$$

in which both g_1 and g_2 are composed of two 3×3 convolutional layer joined by *ReLU*, and they share parameters of the first 3×3 convolution. The parameters of g_1 and g_2 are not shared across different SNblocks in our generator. With our proposed SANorm layer, the object structure and saliency information provided by saliency maps is infused into the generator through adaptively modulating distribution of intermediate features, which improves generator’s ability to maintain image content structure during style translation process.

3.2.2 Saliency Attended Discriminator

Adversarial learning is of kernel importance for style transfer. ChipGAN [34] builds an extra discriminator to learn the specific ink-wash diffusion effect

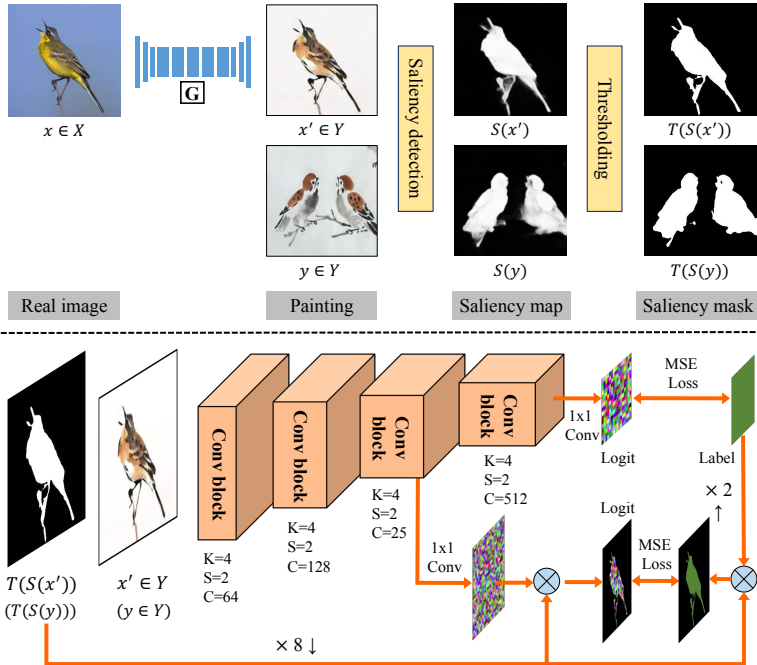


Fig. 6 Architecture details of our proposed saliency attended discriminator. The figure shows the structure of the target-domain discriminator D_Y , which takes either real or generated Chinese ink-wash paintings as input and discriminates between them. The architecture is the same for the source-domain discriminator D_X .

which is mimicked by basic dilation and Gaussian blur operations. We alternatively adopt saliency based attention mechanism to promote ink-wash style rendering quality, which achieves finer stylization effect without introducing extra discriminator network.

Specifically, we propose saliency attended discriminator which is illustrated in Fig. 6. Taking the target-domain discriminator D_Y which distinguishes between real and generated Chinese ink-wash paintings as an example. The discriminator adopts PatchGAN [25] form which outputs a matrix with each element indicating the authenticity score of a corresponding patch in the input image. We design a multi-scale attention-based discriminator architecture which comprises four downsampling convolutional blocks, the details of each block follow the setting of PatchGAN discriminator in Pix2Pix [25]. After the fourth block, feature maps of $\frac{1}{16}$ spatial size are converted to a single-channel logit matrix with a 1×1 convolution, which is then driven to the $\frac{1}{16}$ scale label matrix with MSE loss (we use LSGAN [58] objective function for more stable convergence).

Apart from this main discrimination branch, we also append a saliency based auxiliary branch to examine patch authenticity at more fine-grained

level. Specifically, another 1×1 convolution is used to convert the $\frac{1}{8}$ scale feature maps output by the third convolutional block to a $\frac{1}{8}$ scale logit matrix. Meanwhile, the input painting is detected by the saliency detection model to generate a saliency map highlighting image regions of salient objects. The detected saliency map is bilinearly interpolated to the same $\frac{1}{8}$ scale and thresholded, yielding a binary saliency mask that is multiplied with both the predicted logit matrix in the auxiliary branch and the corresponding $\frac{1}{8}$ scale label matrix. The MSE loss is minimized between these two saliency masked matrices. In this way, as a supplement to the coarse-grained adversarial learning of the main branch, the auxiliary branch focuses adversarial learning attention to more fine-grained patches only around salient objects of images. This contributes to producing finer ink-wash style rendering to salient objects.

3.3 Objective Functions

Our SRAGAN includes three loss functions: saliency attended adversarial loss L_{SAAAdv} , cycle consistency loss L_{cycle} , and saliency IOU loss L_{SIOU} . Below is the formulation of these loss functions.

3.3.1 Saliency Attended Adversarial Loss

The saliency attended adversarial loss L_{SAAAdv} is composed of a generator part $L_{SAAAdv.G}$ and a discriminator part $L_{SAAAdv.D}$, and both two parts can be further decomposed into a $X \rightarrow Y$ item and a $Y \rightarrow X$ one.

$$L_{SAAAdv} = L_{SAAAdv.G}^{X \rightarrow Y} + L_{SAAAdv.G}^{Y \rightarrow X} + L_{SAAAdv.D}^{X \rightarrow Y} + L_{SAAAdv.D}^{Y \rightarrow X}. \quad (5)$$

Taking the $X \rightarrow Y$ mapping as example, let $D_Y^1(\cdot)$ denote the output $\frac{1}{16}$ scale logit matrix at the main branch of D_Y , $D_Y^2(\cdot)$ denote the predicted $\frac{1}{8}$ scale logit matrix at the auxiliary branch, $\mathbb{1}^1$ be an all-one matrix of the same $\frac{1}{16}$ spatial scale as $D_Y^1(\cdot)$, $\mathbb{1}^2$ be an all-one matrix of the same $\frac{1}{8}$ spatial scale as $D_Y^2(\cdot)$, $S(\cdot)$ and $T(\cdot)$ denote saliency detection and thresholding respectively, \downarrow denotes $\frac{1}{8}$ scale downsampling, then:

$$L_{SAAAdv.D}^{X \rightarrow Y} = \mathbb{E}_{y \in Y} \left[\frac{\sum [(D_Y^1(y) - \mathbb{1}^1)^2]}{\sum \mathbb{1}^1} + \frac{\sum [T(S(y)_{\downarrow}) \otimes (D_Y^2(y) - \mathbb{1}^2)^2]}{\sum [T(S(y)_{\downarrow}) \otimes \mathbb{1}^2]} \right] + \mathbb{E}_{x'} \left[\frac{\sum [D_Y^1(x')^2]}{\sum \mathbb{1}^1} + \frac{\sum [T(S(x')_{\downarrow}) \otimes D_Y^2(x')^2]}{\sum [T(S(x')_{\downarrow}) \otimes \mathbb{1}^2]} \right], \quad (6)$$

$$L_{SAAAdv.G}^{X \rightarrow Y} = \mathbb{E}_{x'} \left[\frac{\sum [(D_Y^1(x') - \mathbb{1}^1)^2]}{\sum \mathbb{1}^1} + \frac{\sum [T(S(x')_{\downarrow}) \otimes (D_Y^2(x') - \mathbb{1}^2)^2]}{\sum [T(S(x')_{\downarrow}) \otimes \mathbb{1}^2]} \right], \quad (7)$$

where x' is the generated painting by the saliency regularized generator G given the input real image $x \in X$, i.e., $x' = G(x, S(x))$, \otimes denotes elementwise

multiplication. Similarly, the losses for the inverse $Y \rightarrow X$ mapping is:

$$L_{SAAAdv.D}^{Y \rightarrow X} = \mathbb{E}_{x \in X} \left[\frac{\sum [(D_X^1(x) - \mathbb{1}^1)^2]}{\sum \mathbb{1}^1} + \frac{\sum [T(S(x)_\downarrow) \otimes (D_X^2(x) - \mathbb{1}^2)^2]}{\sum [T(S(x)_\downarrow) \otimes \mathbb{1}^2]} \right] +$$

$$\mathbb{E}_{y'} \left[\frac{\sum [D_X^1(y')^2]}{\sum \mathbb{1}^1} + \frac{\sum [T(S(y')_\downarrow) \otimes D_X^2(y')^2]}{\sum [T(S(y')_\downarrow) \otimes \mathbb{1}^2]} \right], \quad (8)$$

$$L_{SAAAdv.G}^{Y \rightarrow X} = \mathbb{E}_{y'} \left[\frac{\sum [(D_X^1(y') - \mathbb{1}^1)^2]}{\sum \mathbb{1}^1} + \frac{\sum [T(S(y')_\downarrow) \otimes (D_X^2(y') - \mathbb{1}^2)^2]}{\sum [T(S(y')_\downarrow) \otimes \mathbb{1}^2]} \right], \quad (9)$$

where y' is the generated real image by the saliency regularized generator F given the input real painting $y \in Y$, i.e., $y' = F(y, S(y))$.

3.3.2 Cycle Consistency Loss

The cycle consistency loss L_{cycle} enforces mutual invertibility of two saliency regularized generators G and F :

$$L_{cycle} = \mathbb{E}_{x \in X} [\|x - F(G(x, S(x)), S(x))\|_1] +$$

$$\mathbb{E}_{y \in Y} [\|y - G(F(y, S(y)), S(y))\|_1]. \quad (10)$$

3.3.3 Saliency IOU Loss

The saliency IOU loss L_{SSIOU} regularizes object saliency consistency between input images and generated paintings. It maximizes intersection over union between the binary saliency masks of generator inputs and outputs, as well as between saliency masks of generator inputs and cyclically recovered results:

$$L_{SSIOU} = - \mathbb{E}_{x \in X} \left[\frac{T(S(x)) \cap T(S(x'))}{T(S(x)) \cup T(S(x'))} + \frac{T(S(x)) \cap T(S(\hat{x}))}{T(S(x)) \cup T(S(\hat{x}))} \right] -$$

$$\mathbb{E}_{y \in Y} \left[\frac{T(S(y)) \cap T(S(y'))}{T(S(y)) \cup T(S(y'))} + \frac{T(S(y)) \cap T(S(\hat{y}))}{T(S(y)) \cup T(S(\hat{y}))} \right], \quad (11)$$

in which x' is the generated ink-wash painting produced by generator G , i.e., $x' = G(x, S(x))$, \hat{x} is the cyclically reconstructed real image, i.e., $\hat{x} = F(G(x, S(x)), S(x))$. Similarly, $y' = F(y, S(y))$, $\hat{y} = G(F(y, S(y)), S(y))$.

3.3.4 Total Loss

The total loss L_{total} is the weighted combination of component loss functions:

$$L_{total} = \lambda_1 L_{SAAAdv} + \lambda_2 L_{cycle} + \lambda_3 L_{SSIOU}, \quad (12)$$

where the weights λ_1 , λ_2 , and λ_3 control the relative importance of each component loss function to the overall learning objective.

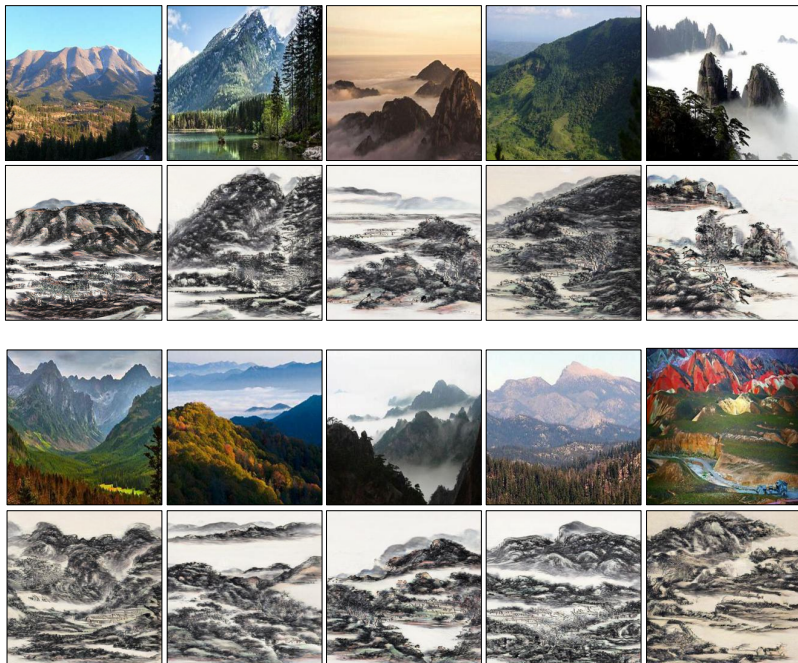


Fig. 7 Example qualitative results of our SRAGAN for converting real landscape photos (the top row) into Chinese ink-wash landscape paintings (the bottom row). Results are evaluated on the test set of the RealLandscape dataset. **Best viewed with zoom in.**

4 Experiments

4.1 Data Preparation

We experiment on generating three types of typical Chinese ink-wash paintings: (i) landscape, (ii) horses, (iii) birds. For landscape task, we use both the source-domain (RealLandscape) and target-domain (InkLandscape) datasets contributed by [34]. For the other two tasks, datasets of source-domain real pictures and target-domain Chinese ink-wash paintings are described below.

- **RealHorses**: source-domain dataset for horses ink-wash painting generation task. It is screened and supplemented based on the corresponding dataset provided by [34]. We remove some abnormal images (about 200) and increase the total number of pictures to 900. The new dataset contains horses with more diversified poses and scales.
- **InkHorses**: target-domain dataset for horses ink-wash painting generation task. It is screened and supplemented based on the corresponding dataset provided by [34]. We remove around 60 abnormal paintings and increase the total number of painting pictures to 500.
- **RealBirds**: source-domain dataset for birds ink-wash painting generation task collected by ourselves. It comprises 900 real bird images including eagles, magpies, swallows, sparrows, orioles, etc.



Fig. 8 Example qualitative results of our SRAGAN for converting real horse pictures (the left column) into Chinese ink-wash horse paintings (the right column). Results are evaluated on the test set of the RealHorses dataset.

- InkBirds: target-domain dataset for birds ink-wash painting generation task collected by ourselves. It contains 500 Chinese ink-wash paintings of birds including eagles, magpies, swallows, sparrows, etc.

4.2 Training Details

For all the three Chinese ink-wash painting generation tasks, the source-domain real-picture datasets are partitioned into a training set and a test set in proportion of 4:1. All images are resized to 256×256 . In Eq. 12, we set $\lambda_1 = 1$, $\lambda_2 = 10$, and set λ_3 to 1 for landscape and horse painting generation tasks and to 2 for bird painting generation task. Two Adam optimizers with momentum parameters $\beta_1 = 0.5$, $\beta_2 = 0.999$ are applied to train our generator networks (G and F) and discriminator networks (D_X and D_Y) separately. The training phase includes 200 epochs with learning rate of both two optimizers fixed at 0.0002 in the first 100 epochs and then linearly decayed to 0 in the next 100 epochs. The generator part (G and F) and the discriminator part (D_X and D_Y) are alternatively trained with the former one optimized with objective function of $\lambda_1(L_{SAAdv_G}^{X \rightarrow Y} + L_{SAAdv_G}^{Y \rightarrow X}) + \lambda_2 L_{cycle} + \lambda_3 L_{SSIOU}$ and the latter one optimized by minimizing $\lambda_1(L_{SAAdv_D}^{X \rightarrow Y} + L_{SAAdv_D}^{Y \rightarrow X})$.



Fig. 9 Example qualitative results of our SRGAN for converting real bird pictures (the top row) into Chinese ink-wash bird paintings (the bottom row). Results are evaluated on the test set of the RealBirds dataset. **Better to zoom in for higher resolution.**

4.3 Qualitative Evaluation

The example evaluation results of our SRGAN for Chinese ink-wash landscape painting, horse painting, and bird painting generation task are displayed in Fig. 7, Fig. 8, and Fig. 9 respectively. Our method produces paintings with precise ink-wash style, relatively intact content structure, and prominent visual saliency for salient objects of images.

Qualitative comparisons of our method with related advanced models are demonstrated in Fig. 10 and Fig. 11. Among the compared baseline methods, NST fails to learn the exact ink-wash texture pattern but only transfers superficial color distribution. Results of CUT and GcGAN show noticeable artifacts and missing of content details, indicating the issue of weak content integrity. DistanceGAN generates paintings with coarse and messy brush strokes, which do not reflect the target ink-wash textures. CycleGAN captures relatively precise painting style, but is limited in preserving fine structures of objects. ChipGAN improves model capability of preserving object outlines by virtue of edge prediction loss. However, it still has difficulty in generating fine structures inside object contours. For example, some inner regions of objects in

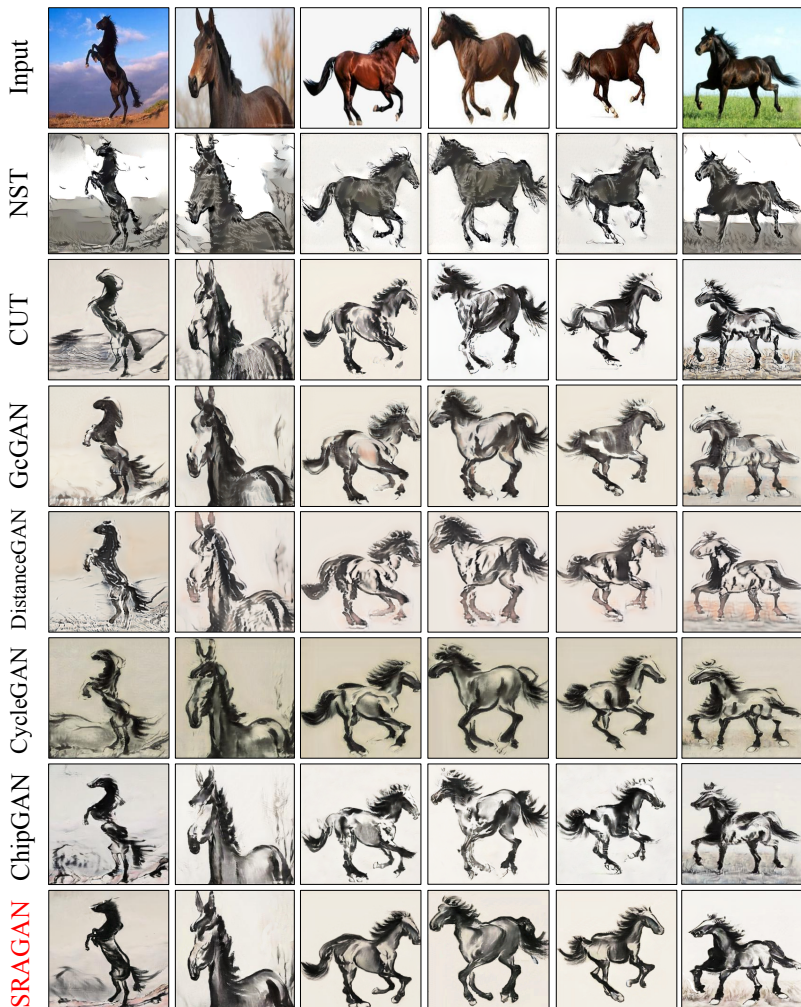


Fig. 10 Qualitative comparison of our SRAGAN with related methods in Chinese ink-wash horse painting generation task. Our method achieves both higher content integrity and stylization quality. **Better to zoom in for higher resolution.**

the generated paintings are void or not visually salient. Moreover, since Chinese ink-wash painting has its unique brushwork skills to portray objects, the drawn objects usually do not strictly match with the source photo objects in contour pixel location. Enforcing pixel-wise contour consistency could thus degrade transfer of typical brush stroke styles. By contrast, our method produces paintings with more fine structures of the objects preserved, and also present higher-quality ink-wash style rendering, thanks to our saliency based content regularization and saliency attended adversarial learning. By maximizing IOU between image saliency masks, our method only constrains object's

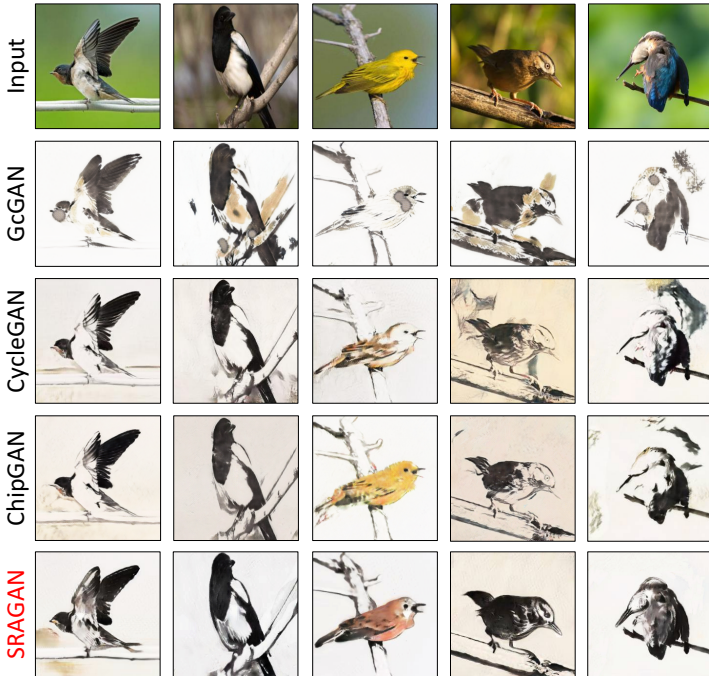


Fig. 11 Qualitative comparison of our SRAGAN with related methods in Chinese ink-wash bird painting generation task. Our method achieves noticeably higher content integrity.

overall structure consistency with mild shift of object contours allowed. Such relaxation is beneficial to produce more delicate ink-wash brush strokes.

4.4 Quantitative Evaluation

Quantitative comparison of our SRAGAN with related methods in FID evaluated on the test set of different datasets is demonstrated in Tab. 1. The FID metric measures the distance of distribution between image set of real Chinese ink-wash paintings and the generated paintings. The lower the FID is, the closer the generated paintings are to the real ones, and thus the better performance of the models. As Tab. 1 shows, the FID values of neural style transfer based methods [9, 20, 23, 43] are substantially higher than GAN based image-to-image translation methods. This is because style transfer methods model image style as low-level textures, which is insufficient to capture the precise ink-wash styles. Among the various GAN based unsupervised image-to-image translation models, our method achieves the lowest FID on all Chinese ink-wash painting generation tasks, due to advantages of our saliency regularized and attended generative adversarial learning. In horse and bird tracks, our method achieves lower FID than related methods by a large margin, while in landscape track, our method only narrowly surpasses CycleGAN and ChipGAN in FID. This is because landscape photos do not have objects with much



Fig. 12 Qualitative ablation study on the key ingredients of our model, including the saliency IOU loss L_{SIOU} , saliency adaptive normalization SANorm, and the saliency attended adversarial loss L_{SAdv} . **Better to zoom in for higher resolution.**

visual saliency as horse or bird pictures, such that the strengths of our saliency based approaches are not fully displayed.

Moreover, we also use the saliency detection and thresholding pipeline to obtain saliency masks for both input real-world pictures and the stylized ink-wash paintings, and calculate the mean IOU (which we denote as Saliency MIOU) between the two domains, to evaluate the degree of object structure integrity after ink-wash stylization. Results reported in Tab. 1 show that, compared with GAN based models, style transfer methods achieve relatively higher Saliency MIOU, namely better object structure integrity, at the expense of relatively superficial stylization degree. Even so, our method achieves the highest score on all datasets, demonstrating the effectiveness of our proposed saliency regularization approaches in promoting object structure integrity.



Fig. 13 Qualitative comparison between pixel-wise saliency loss L_{SMSE} and our proposed saliency IOU loss L_{SIOU} . **Better to zoom in for higher resolution.**

Table 1 Quantitative method comparison on different datasets.

Method	Frechet Inception Distance (FID) ↓			Saliency MIOU ↑		
	Landscape	Horse	Bird	Landscape	Horse	Bird
NST[9]	177.43	186.78	204.95	0.773	0.790	0.828
LapStyle[20]	153.54	179.33	191.98	0.778	0.805	0.801
SANet[23]	148.67	168.25	188.66	0.785	0.812	0.833
Adaattn[43]	142.86	165.95	182.79	0.790	0.814	0.824
CUT[50]	90.56	98.86	124.67	0.702	0.696	0.604
GeGAN[48]	93.17	100.24	146.86	0.716	0.685	0.577
DistanceGAN[49]	135.20	144.82	171.25	0.647	0.516	0.483
CycleGAN[31]	85.85	91.43	115.17	0.766	0.747	0.764
UNIT[47]	88.24	89.55	112.46	0.772	0.755	0.780
DITR[32]	89.06	91.98	118.06	0.747	0.750	0.769
ChipGAN[34]	85.94	86.67	110.38	0.774	0.779	0.793
SRAGAN (ours)	85.28	82.51	104.96	0.793	0.820	0.841

Note: The “Landscape”, “Horse”, “Bird” denote the test set of the RealLandscape, RealHorses, RealBirds dataset, respectively.

Besides, user study is conducted to evaluate models from subjective perspective. For all the three types of ink-wash painting generation tasks, we randomly sample 50 pictures from the corresponding test set, on which our method as well as related competitive models are evaluated. For each task, 30 participants are invited to score the generated paintings of each method with 1-10 integer scores from the perspective of structure integrity and ink-wash style quality, then the final scores of these two aspects are calculated by averaging across all participants and test pictures. The overall preference score is the average value of the structure integrity score and the ink-wash style quality score. Results of the above user study are displayed in Fig. 14. Our method

Table 2 Quantitative ablation study on key ingredients of our method.

Ablation	Frechet Inception Distance (FID) ↓			Saliency MIOU ↑		
	Landscape	Horse	Bird	Landscape	Horse	Bird
w/o L_{SIOU}	85.62	86.20	111.35	0.781	0.781	0.799
w/ L_{SMSE}	86.47	85.78	109.40	0.798	0.834	0.850
w/o SA_{Norm}	85.40	85.54	108.28	0.789	0.807	0.832
w/o L_{SAAdv}	85.35	84.13	106.23	0.794	0.831	0.842
SRAGAN (ours)	85.28	82.51	104.96	0.793	0.820	0.841

achieves the top user scores in both content integrity and style quality, which is basically in line with the quantitative results in Tab. 1.

4.5 Ablation Study

To investigate the effectiveness of the key ingredients of our method, we design ablation studies with notations explained as follows:

- w/o L_{SIOU} : the model without saliency IOU loss.
- w/o SA_{Norm} : the model without saliency adaptive normalization (SA_{Norm}) layers, i.e., all SN_{blocks} in the generator are replaced with normal Resblocks.
- w/o L_{SAAdv} : the model without saliency attended adversarial loss, namely, the proposed saliency attended discriminator is replaced with the normal PatchGAN discriminator [25] optimized with the basic LSGAN [58] loss.
- w/ L_{SMSE} : the model that replaces the proposed saliency IOU loss L_{SIOU} with saliency MSE loss L_{SMSE} which minimizes pixel-wise mean squared error between the extracted binary saliency masks.

As shown in Fig. 12, the absence of L_{SIOU} leads to the stylized objects with noticeable missing of content details or loss of structure integrity. The same issue also appears for the case of w/o SA_{Norm} but less obvious than w/o L_{SIOU} . These reflect the importance of our proposed explicit and implicit saliency regularizations in stylizing objects with high content integrity. Comparing the results of w/o L_{SAAdv} to the results of the full model, it shows that our proposed saliency attended adversarial learning is capable of generating finer ink-wash textures and brush strokes for salient objects. Under our saliency regularizations, the normal adversarial loss produces results with relatively rigid stylization effect, whereas results of our L_{SAAdv} exhibit more delicate ink-wash style patterns. By combining the saliency regularizations and the saliency attended adversarial learning, the ultimate full model can balance content and style satisfactorily. In Fig. 13, we qualitatively demonstrate the superiority of our L_{SIOU} over directly minimizing the MSE between saliency masks, i.e., L_{SMSE} . Results show that the pixel-wise constraint of L_{SMSE} is too strong to enable generation of fine structures with sufficient brushwork characteristics of Chinese ink-wash paintings. Our SIOU loss, by contrast, enforces only objects’ overall structure similarity, and thus allows for generating more vivid and delicate brush strokes at the expense of mild shift of object outlines.

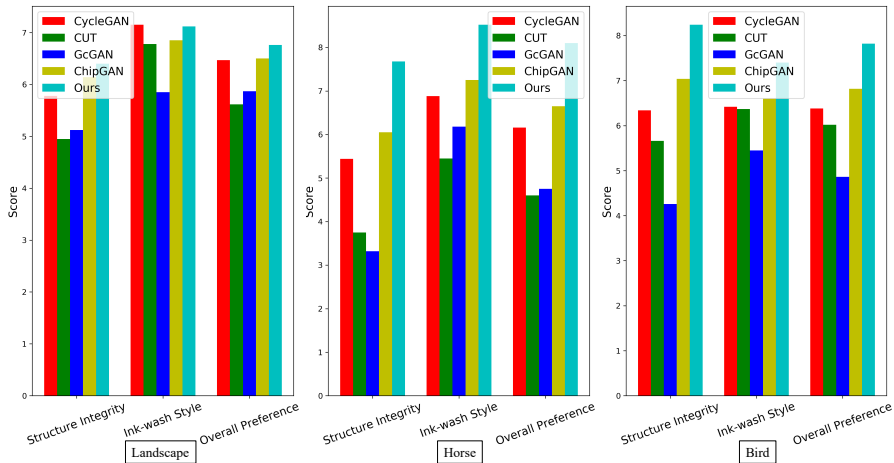


Fig. 14 User study of related methods evaluated on different datasets.

We also conduct quantitative ablation study in terms of FID and Saliency MIOU, results are displayed in Tab. 2. It shows that both the saliency IOU loss and the saliency adaptive normalization have evident contributions in promoting Saliency MIOU, i.e., improving structure integrity of the stylized objects. These two regularization approaches also play a critical role in improving FID, especially for horse and bird tracks, due to their effectiveness in alleviating object content corruption issue. The introduction of saliency attended adversarial learning also brings consistent improvement in FID, at the cost of slight drop in Saliency MIOU. Compared with our saliency IOU loss, using saliency MSE loss leads to noticeable improvement in content consistency, but yields worse FID since pixel-wise consistency constraint confines model’s ability to produce vivid and delicate ink-wash style elements.

5 Conclusion

This paper proposes SRAGAN, which combines saliency detection with unsupervised image-to-image translation for Chinese ink-wash painting style transfer. In SRAGAN, saliency based regularization approaches are proposed to tackle content corruption issue, including saliency IOU loss and saliency adaptive normalization module. Moreover, a saliency based adversarial learning approach is proposed, which utilizes saliency detection to focus adversarial learning attention onto salient objects of images, allowing for rendering the objects with finer ink-wash style elements. Superiorities of our method in both content integrity and stylization quality of the generated Chinese ink-wash paintings are fully displayed with extensive experiments.

Acknowledgments. This work has been partially supported by grants from: National Natural Science Foundation of China (No. 12071458, 71731009)

References

- [1] Wu Y H, Liu Y, Zhan X, et al. P2T: Pyramid pooling transformer for scene understanding[J]. *IEEE Transactions on Pattern Analysis and Machine Intelligence*, 2022.
- [2] Ju C, Han T, Zheng K, et al. Prompting visual-language models for efficient video understanding[C]//*European Conference on Computer Vision*. Springer, Cham, 2022: 105-124.
- [3] Carion N, Massa F, Synnaeve G, et al. End-to-end object detection with transformers[C]//*European conference on computer vision*. Springer, Cham, 2020: 213-229.
- [4] Zhu X, Su W, Lu L, et al. Deformable DETR: Deformable Transformers for End-to-End Object Detection[C]//*International Conference on Learning Representations*. 2020.
- [5] Strudel R, Garcia R, Laptev I, et al. Segmenter: Transformer for semantic segmentation[C]//*Proceedings of the IEEE/CVF International Conference on Computer Vision*. 2021: 7262-7272.
- [6] Liang J, Homayounfar N, Ma W C, et al. Polytransform: Deep polygon transformer for instance segmentation[C]//*Proceedings of the IEEE/CVF Conference on Computer Vision and Pattern Recognition*. 2020: 9131-9140.
- [7] Zamir S W, Arora A, Khan S, et al. Restormer: Efficient transformer for high-resolution image restoration[C]//*Proceedings of the IEEE/CVF Conference on Computer Vision and Pattern Recognition*. 2022: 5728-5739.
- [8] Tu Z, Talebi H, Zhang H, et al. Maxim: Multi-axis mlp for image processing[C]//*Proceedings of the IEEE/CVF Conference on Computer Vision and Pattern Recognition*. 2022: 5769-5780.
- [9] Gatys L A, Ecker A S, Bethge M. Image style transfer using convolutional neural networks[C]//*Proceedings of the IEEE conference on computer vision and pattern recognition*. 2016: 2414-2423.
- [10] Goodfellow I, Pouget-Abadie J, Mirza M, et al. Generative adversarial networks[J]. *Communications of the ACM*, 2020, 63(11): 139-144.
- [11] Li S, Xu X, Nie L, et al. Laplacian-steered neural style transfer[C]//*Proceedings of the 25th ACM international conference on Multimedia*. 2017: 1716-1724.
- [12] Liu X C, Cheng M M, Lai Y K, et al. Depth-aware neural style transfer[C]//*Proceedings of the Symposium on Non-Photorealistic Animation and Rendering*. 2017: 1-10.

- [13] Kolkin N, Salavon J, Shakhnarovich G. Style transfer by relaxed optimal transport and self-similarity[C]//Proceedings of the IEEE/CVF Conference on Computer Vision and Pattern Recognition. 2019: 10051-10060.
- [14] Johnson J, Alahi A, Fei-Fei L. Perceptual losses for real-time style transfer and super-resolution[C]//European conference on computer vision. Springer, Cham, 2016: 694-711.
- [15] Ulyanov D, Lebedev V, Vedaldi A, et al. Texture networks: Feed-forward synthesis of textures and stylized images[J]. arXiv preprint arXiv:1603.03417, 2016.
- [16] Chen D, Yuan L, Liao J, et al. Stylebank: An explicit representation for neural image style transfer[C]//Proceedings of the IEEE conference on computer vision and pattern recognition. 2017: 1897-1906.
- [17] Dumoulin V, Shlens J, Kudlur M. A learned representation for artistic style[J]. arXiv preprint arXiv:1610.07629, 2016.
- [18] Li Y, Fang C, Yang J, et al. Diversified texture synthesis with feed-forward networks[C]//Proceedings of the IEEE conference on computer vision and pattern recognition. 2017: 3920-3928.
- [19] Zhang H, Dana K. Multi-style generative network for real-time transfer[C]//Proceedings of the European Conference on Computer Vision (ECCV) Workshops. 2018: 0-0.
- [20] Lin T, Ma Z, Li F, et al. Drafting and revision: Laplacian pyramid network for fast high-quality artistic style transfer[C]//Proceedings of the IEEE/CVF Conference on Computer Vision and Pattern Recognition. 2021: 5141-5150.
- [21] Wang X, Wang W, Yang S, et al. CLAST: Contrastive Learning for Arbitrary Style Transfer[J]. IEEE Transactions on Image Processing, 2022.
- [22] Chen H, Wang Z, Zhang H, et al. Artistic style transfer with internal-external learning and contrastive learning[J]. Advances in Neural Information Processing Systems, 2021, 34: 26561-26573.
- [23] Park D Y, Lee K H. Arbitrary style transfer with style-attentional networks[C]//proceedings of the IEEE/CVF conference on computer vision and pattern recognition. 2019: 5880-5888.
- [24] Elgammal A, Liu B, Elhoseiny M, et al. Can: Creative adversarial networks, generating” art” by learning about styles and deviating from style norms[J]. arXiv preprint arXiv:1706.07068, 2017.

- [25] Isola P, Zhu J Y, Zhou T, et al. Image-to-image translation with conditional adversarial networks[C]//Proceedings of the IEEE conference on computer vision and pattern recognition. 2017: 1125-1134.
- [26] Wang L, Sindagi V, Patel V. High-quality facial photo-sketch synthesis using multi-adversarial networks[C]//2018 13th IEEE international conference on automatic face & gesture recognition (FG 2018). IEEE, 2018: 83-90.
- [27] Zhang S, Ji R, Hu J, et al. Robust Face Sketch Synthesis via Generative Adversarial Fusion of Priors and Parametric Sigmoid[C]//IJCAI. 2018: 1163-1169.
- [28] Yi R, Liu Y J, Lai Y K, et al. Apdrawinggan: Generating artistic portrait drawings from face photos with hierarchical gans[C]//Proceedings of the IEEE/CVF Conference on Computer Vision and Pattern Recognition. 2019: 10743-10752.
- [29] Sanakoyeu A, Kotovenko D, Lang S, et al. A style-aware content loss for real-time hd style transfer[C]//proceedings of the European conference on computer vision (ECCV). 2018: 698-714.
- [30] Kotovenko D, Sanakoyeu A, Ma P, et al. A content transformation block for image style transfer[C]//Proceedings of the IEEE/CVF Conference on Computer Vision and Pattern Recognition. 2019: 10032-10041.
- [31] Zhu J Y, Park T, Isola P, et al. Unpaired image-to-image translation using cycle-consistent adversarial networks[C]//Proceedings of the IEEE international conference on computer vision. 2017: 2223-2232.
- [32] Lee H Y, Tseng H Y, Huang J B, et al. Diverse image-to-image translation via disentangled representations[C]//Proceedings of the European conference on computer vision (ECCV). 2018: 35-51.
- [33] Anoosheh A, Agustsson E, Timofte R, et al. Combogan: Unrestrained scalability for image domain translation[C]//Proceedings of the IEEE conference on computer vision and pattern recognition workshops. 2018: 783-790.
- [34] He B, Gao F, Ma D, et al. Chipgan: A generative adversarial network for chinese ink wash painting style transfer[C]//Proceedings of the 26th ACM international conference on Multimedia. 2018: 1172-1180.
- [35] Xie S, Tu Z. Holistically-nested edge detection[C]//Proceedings of the IEEE international conference on computer vision. 2015: 1395-1403.

- [36] Gao S H, Tan Y Q, Cheng M M, et al. Highly efficient salient object detection with 100k parameters[C]//European Conference on Computer Vision. Springer, Cham, 2020: 702-721.
- [37] Huang X, Belongie S. Arbitrary style transfer in real-time with adaptive instance normalization[C]//Proceedings of the IEEE international conference on computer vision. 2017: 1501-1510.
- [38] Li Y, Wang N, Liu J, et al. Demystifying neural style transfer[J]. arXiv preprint arXiv:1701.01036, 2017.
- [39] Kolkin N, Salavon J, Shakhnarovich G. Style transfer by relaxed optimal transport and self-similarity[C]//Proceedings of the IEEE/CVF Conference on Computer Vision and Pattern Recognition. 2019: 10051-10060.
- [40] Li C, Wand M. Combining markov random fields and convolutional neural networks for image synthesis[C]//Proceedings of the IEEE conference on computer vision and pattern recognition. 2016: 2479-2486.
- [41] Mechrez R, Talmi I, Zelnik-Manor L. The contextual loss for image transformation with non-aligned data[C]//Proceedings of the European conference on computer vision (ECCV). 2018: 768-783.
- [42] Li Y, Fang C, Yang J, et al. Universal style transfer via feature transforms[J]. Advances in neural information processing systems, 2017, 30.
- [43] Liu S, Lin T, He D, et al. Adaattn: Revisit attention mechanism in arbitrary neural style transfer[C]//Proceedings of the IEEE/CVF international conference on computer vision. 2021: 6649-6658.
- [44] Zhang Y, Tang F, Dong W, et al. Domain Enhanced Arbitrary Image Style Transfer via Contrastive Learning[J]. arXiv preprint arXiv:2205.09542, 2022.
- [45] Jiang Y, Lian Z, Tang Y, et al. DCFont: an end-to-end deep Chinese font generation system[M]//SIGGRAPH Asia 2017 Technical Briefs. 2017: 1-4.
- [46] Jiang Y, Lian Z, Tang Y, et al. Sfont: Structure-guided chinese font generation via deep stacked networks[C]//Proceedings of the AAAI conference on artificial intelligence. 2019, 33(01): 4015-4022.
- [47] Liu M Y, Breuel T, Kautz J. Unsupervised image-to-image translation networks[J]. Advances in neural information processing systems, 2017, 30.
- [48] Fu H, Gong M, Wang C, et al. Geometry-consistent generative adversarial networks for one-sided unsupervised domain mapping[C]//Proceedings of

the IEEE/CVF Conference on Computer Vision and Pattern Recognition. 2019: 2427-2436.

- [49] Benaim S, Wolf L. One-sided unsupervised domain mapping[J]. *Advances in neural information processing systems*, 2017, 30.
- [50] Park T, Efros A A, Zhang R, et al. Contrastive learning for unpaired image-to-image translation[C]//*European conference on computer vision*. Springer, Cham, 2020: 319-345.
- [51] Chang H, Lu J, Yu F, et al. Pairedcyclegan: Asymmetric style transfer for applying and removing makeup[C]//*Proceedings of the IEEE conference on computer vision and pattern recognition*. 2018: 40-48.
- [52] Gu Q, Wang G, Chiu M T, et al. Ladvn: Local adversarial disentangling network for facial makeup and de-makeup[C]//*Proceedings of the IEEE/CVF International Conference on Computer Vision*. 2019: 10481-10490.
- [53] Organisciak D, Ho E S L, Shum H P H. Makeup style transfer on low-quality images with weighted multi-scale attention[C]//*2020 25th International Conference on Pattern Recognition (ICPR)*. IEEE, 2021: 6011-6018.
- [54] Gao X, Tian Y, Qi Z. RPD-GAN: Learning to draw realistic paintings with generative adversarial network[J]. *IEEE Transactions on Image Processing*, 2020, 29: 8706-8720.
- [55] Chen Y, Lai Y K, Liu Y J. Cartoongan: Generative adversarial networks for photo cartoonization[C]//*Proceedings of the IEEE conference on computer vision and pattern recognition*. 2018: 9465-9474.
- [56] Wang X, Yu J. Learning to cartoonize using white-box cartoon representations[C]//*Proceedings of the IEEE/CVF conference on computer vision and pattern recognition*. 2020: 8090-8099.
- [57] Gao X, Zhang Y, Tian Y. Learning to Incorporate Texture Saliency Adaptive Attention to Image Cartoonization[C]//*International Conference on Machine Learning*. PMLR, 2022: 7183-7207.
- [58] Mao X, Li Q, Xie H, et al. Least squares generative adversarial networks[C]//*Proceedings of the IEEE international conference on computer vision*. 2017: 2794-2802.